

On Fingering Instability in Immiscible Displacement

Alexander Babchin* Irina Brailovsky† Peter Gordon ‡
Gregory Sivashinsky§

December 23, 2007

Abstract

Departing from the classical Buckley-Leverett theory for two-phase immiscible flows in porous media, a reduced evolution equation for the water-oil displacement front is formulated and studied numerically. The reduced model successfully reproduces the basic features of the finger-forming dynamics observed in recent direct numerical simulations.

PACS numbers: *47.20.Gv, 47.20.Ky, 47.20.Ma*

Key words: viscous fingers, immiscible displacement, two-phase flows

1 Introduction

In oil extraction engineering it is common practice to inject water into the oil field at certain points in an attempt to drive oil to certain other spots for pumping. In large reservoirs the oil displacement by water-flooding often assumes the form of an advancing front, a moving zone of limited extent across which the saturation of water (the fraction of pore space occupied by water) changes rapidly compared to regions of nearly constant saturation upstream and downstream. In this process the phenomenon of fingering has long been identified. The water, meant to push the oil forward, tends to penetrate the oil through spontaneously formed channels (fingers) [1]. The mechanism triggering the fingering is physically akin to that of the well-studied Saffman-Taylor (ST) problem dealing with the displacement of a viscous fluid by a less viscous one in Hele-Shaw cell, a pair of parallel glass plates separated by a narrow gap [2]. In both systems the instability is caused by the high mobility of the displacing fluid, which results in similar dispersion relations in the long-wavelength range where the impact of capillary forces is negligible. The capillary forces, however, are needed to ensure relaxation of the short-wavelength disturbances and to make the associated evolution problem dynamically well-posed, that is free of pathological instabilities.

*Heavy Oil and Oil Sands, Alberta Research Council, Edmonton, AL T6N1E4, Canada; babchin@arc.ab.ca

†Department of Mathematical Sciences, Tel Aviv University, Tel Aviv 69978, Israel; brailir@post.tau.ac.il

‡Department of Mathematical Sciences, New Jersey Institute of Technology, Newark, NJ 07102 USA; peterg@njit.edu, corresponding author

§Department of Mathematical Sciences, Tel Aviv University, Tel Aviv 69978, Israel; grishas@post.tau.ac.il

In the ST problem, accounting for the capillary forces is readily achieved by relating the pressure jump at the interface to its curvature and the surface tension (Laplace’s law). For the displacement in porous media the matter is more involved. Here the interplay between the flow-field and capillary forces is, as a rule, described by the Buckley-Leverett theory for immiscible two-phase flow, where the saturation front acquires a finite-width structure. This feature, however, turns even the linear-stability analysis into a technically difficult problem which can be tackled only approximately or numerically [3],[4],[5],[6],[7],[8],[9].

The long-wavelength stability analysis presented in Barenblatt et al [3],[4] showed that correction to the perturbation of the displacement front normal velocity is proportional to its second-order arc-length derivative, which ensures relaxation of short-wavelength disturbances. Recently in Brailovsky et al [10] this observation has been utilized in formulation of an heuristic free-interface model, where the normal velocity of the front was considered as a linear function of its curvature. Yet, a more systematic analysis of the problem conducted in the present study shows that the relation between the normal velocity of the front and its local geometry is of a somewhat different nature. It transpires that the short-wavelength relaxation is actually provided not by the front curvature, but rather by its ‘stretch’ induced by the underlying flow-field. It is curious that the curvature based model is still functionally valid, but, as has been recently shown [11], for the miscible rather than immiscible displacement.

2 The Buckley-Leverett model

The incompressible flow of two immiscible fluids in porous medium can be described by the the following system of equations [4],

$$\phi S_t + \mathbf{u} \cdot \nabla F(S) = \nabla \cdot (D(S)\nabla S), \quad (1)$$

$$\mathbf{u} = -\lambda(S)\nabla P, \quad (2)$$

$$\nabla \cdot \mathbf{u} = 0. \quad (3)$$

Equation (1) is known as the Buckley-Leverett equation, Eq. (2) is Darcy’s law, and Eq.(3) expresses incompressibility. Here S is the saturation of the wetting (water) phase.

$$\mathbf{u} = \mathbf{u}_w + \mathbf{u}_o \quad (4)$$

is the total velocity of the two-phase flow, where the subscripts w and o denote water and oil phases respectively.

$$P = p_w F(S) + p_o(1 - F(S)) - \int_S^1 p_c(v)F'_v(v)dv \quad (5)$$

is the mean pressure of the two-phase flow. p_w and p_o are the pressure of the phases.

$$p_c(S) = p_o - p_w \quad (6)$$

is the capillarity pressure.

$$p_c(S) = \sigma \sqrt{\frac{\phi}{K}} J(S), \quad (7)$$

where σ is the surface tension, ϕ and K are porosity and permeability of the porous medium, respectively. $J(S)$ is known as the Leverett function.

$$F(S) = \frac{\mu_o}{k_{ro}(S)} \left(\frac{\mu_w}{k_{rw}(S)} + \frac{\mu_o}{k_{ro}(S)} \right)^{-1} \quad (8)$$

is the fractional flow function, where μ_w , μ_o are dynamic viscosities and k_{rw} , k_{ro} are relative permeabilities of the phases.

$$\lambda(S) = K \left(\frac{k_{rw}(S)}{\mu_w} + \frac{k_{ro}(S)}{\mu_o} \right) \quad (9)$$

is the total mobility of the two-phase flow.

$$D(S) = -K \frac{dp_c}{dS} \left(\frac{\mu_w}{k_{rw}(S)} + \frac{\mu_o}{k_{ro}(S)} \right)^{-1} \quad (10)$$

is the capillary diffusivity.

For brevity the further discussion is restricted to two dimensions. Results of the extension to three dimensions are outlined in the Appendix.

3 One-dimensional displacement and its stability

For further discussion it is helpful to reproduce some basic results on the steady planar saturation wave driven by a uniform flow-field $\mathbf{u} = (U_\infty, 0)$. In this geometry,

$$S(x, t) = S(x - Vt), \quad (11)$$

where V is the wave velocity (to be determined). Setting

$$x - Vt = \chi, \quad (12)$$

Eq. (1) becomes

$$-\phi V S_\chi + U_\infty (F(S))_\chi = (D(S) S_\chi)_\chi. \quad (13)$$

The global integration of Eq. (13) then readily yields,

$$\phi V = \left(\frac{F_b - F_a}{S_b - S_a} \right) U_\infty, \quad (14)$$

where,

$$S_a = S(\chi \rightarrow +\infty), \quad S_b = S(\chi \rightarrow -\infty), \quad S_b > S_a, \quad (15)$$

and

$$F_a = F(S_a), \quad F_b = F(S_b), \quad F_b > F_a. \quad (16)$$

The pressure profile $P(\chi)$ is determined from Eq. (2). For the relation (14) to be meaningful the line between the points (S_a, F_a) and (S_b, F_b) should not intersect the fractional flow curve $F(S)$ between S_a and S_b [12]. For a given saturation S_a this condition defines the range of velocities V allowed for sustaining the saturation wave of a permanent structure. The location of the saturation front may be specified as a point $\chi = \chi_f$ where,

$$\int_{-\infty}^{\infty} (\chi - \chi_f) \frac{dS}{d\chi} d\chi = 0, \quad (17)$$

assuming that the integral converges.

The mobility drop across the wave ($d\lambda/d\chi < 0$) renders the one-dimensional displacement unstable to transversal perturbations. The long-wavelength stability analysis conducted for the mild mobility-contrast yields the following dispersion relation (Barenblatt et al [3],[4]),

$$\phi\omega = \left(\frac{F_b - F_a}{S_b - S_a} \right) \left(\frac{\lambda_b - \lambda_a}{\lambda_b + \lambda_a} \right) U_\infty |k| - \left(\frac{G_b - G_a}{S_b - S_a} \right) k^2, \quad (18)$$

where ω is the instability growth rate, k is the perturbation wave-number,

$$G_b - G_a = \int_{S_a}^{S_b} D(S) dS, \quad (19)$$

and

$$\lambda_b = \lambda(S_b), \quad \lambda_a = \lambda(S_a), \quad \lambda_b > \lambda_a. \quad (20)$$

The first term on the right provides the long-wavelength instability, while the second ensures dissipation of short-wavelength disturbances due to capillary forces.

4 Sharp interface limit and free-boundary formulation

Assume that initially the saturation front is weakly curved, that is $\mathcal{K} \sim \varepsilon$, where \mathcal{K} is the front curvature and $\varepsilon \ll 1$. In this situation, one may expect that the spatio-temporal structure of the corresponding solution of the problem (1),(2),(3) will involve the short-range variable, associated with the diffusive width of the evolving saturation wave, and long-range variables associated with the curved interface and the flow-field away from the interface. At small ε the model (1),(2),(3) becomes a typical multiple-scale system which can be tackled by a standard machinery of matched asymptotic expansions. The resulting solution, however, involves cumbersome integrals whose physical origin is difficult to trace due to the heavy algebra involved. As in [3],[4], in the present study we therefore restrict the discussion to the limit of mild mobility-contrast,

$$|\lambda - \bar{\lambda}| \ll \bar{\lambda}, \quad \bar{\lambda} = \frac{1}{2}(\lambda_a + \lambda_b), \quad (21)$$

greatly simplifying calculations as well as final relations. It is, however, hoped that the results obtained will provide an adequate dynamical picture for a realistic parameter range well beyond the adopted limit. The immediate technical advantage of this strategy is that for the leading order asymptotics the hydrodynamic problem (2),(3) uncouples from the saturation dynamics. When tackling Eq.(1) we may therefore regard the flow-field as prescribed and involving only long-range variables. Applying standard asymptotic machinery (see Appendix for details) one ends up with the following equation coupling normal velocity of the interface with the divergence-free flow,

$$\phi V_n = \left(\frac{F_b - F_a}{S_b - S_a} \right) \bar{u}_n + \left(\frac{G_b - G_a}{S_b - S_a} \right) \frac{\partial}{\partial s} \left(\frac{\bar{u}_s}{\bar{u}_n} \right). \quad (22)$$

Here, V_n is the normal velocity of the interface, \bar{u}_n and \bar{u}_s are the normal and tangent components of the flow-field evaluated at the interface, and s is the arclength of the interface.

Eq. (22) effectively replaces the Buckley-Leverett equation (1) in the small curvature limit. For a prescribed flow-field \mathbf{u} Eq.(22) defines a second-order differential equation in which the second term on the right ensures dissipation of short-wavelength corrugations, rendering the associated initial-value problem well-posed.

In terms of the interfacial pressure, $\bar{P}(s, t) = P(n = 0, s, t)$, Eq. (22) reads,

$$\phi V_n = \left(\frac{F_b - F_a}{S_b - S_a} \right) \bar{u}_n - \bar{\lambda} \left(\frac{G_b - G_a}{S_b - S_a} \right) \frac{\partial}{\partial s} \left(\frac{1}{\bar{u}_n} \frac{\partial \bar{P}}{\partial s} \right). \quad (23)$$

Eq.(23), derived for the constant mobility ($\lambda = \bar{\lambda}$) will now be iteratively applied to the system where in the far-field variables λ jumps across the interface,

$$\lambda = \lambda_b, \quad n < 0, \quad \text{and} \quad \lambda = \lambda_a, \quad n > 0, \quad (24)$$

while the pressure remains continuous. Recall that due to Eqs. (2) and (3),

$$\nabla \cdot (\lambda \nabla P) = 0. \quad (25)$$

Continuity of the pressure implies discontinuity of the tangential velocity $\bar{u}_s = -\lambda^{-1} \partial_s \bar{P} / \partial s$ at $\lambda_a \neq \lambda_b$.

The problem (25),(24) may be solved within a framework of the theory of the logarithmic potential, allowing to connect the shape of the interface with the normal velocity \bar{u}_n appearing in Eq.(23), see [10],[11] for details.

In this paper the discussion is restricted to two geometrical situations: the displacement front as a closed curve sustained by a point-source of a prescribed intensity Q ,

$$\mathbf{u} = \frac{Q}{2\pi} \frac{\mathbf{r}}{|\mathbf{r}|^2} \quad (26)$$

and displacement in a channel ($0 < x < l, -\infty < y < \infty$) with periodic boundary conditions at the walls and a prescribed constant velocity field at $y \rightarrow \pm\infty$,

$$\mathbf{u}(x, y \rightarrow \pm\infty, t) = \mathbf{U}_\infty = (0, U_\infty). \quad (27)$$

For the point-source geometry the problem (2),(24),(25) yields,

$$P(\mathbf{r}, t) = -\frac{Q}{2\pi\lambda_b} \ln |\mathbf{r}| - \frac{1}{2\pi} \left(\frac{1}{\lambda_a} - \frac{1}{\lambda_b} \right) \int_{\mathcal{L}} \bar{u}_n(t, \hat{\mathbf{r}}) \ln |\mathbf{r} - \hat{\mathbf{r}}| d\mathcal{L}_{\hat{\mathbf{r}}}, \quad (28)$$

$$\begin{aligned} \frac{Q}{2\pi\lambda_b} \frac{\mathbf{r} \cdot \mathbf{N}}{|\mathbf{r}|^2} &= \frac{1}{2} \left(\frac{1}{\lambda_a} + \frac{1}{\lambda_b} \right) \bar{u}_n(\mathbf{r}, t) \\ &- \frac{1}{2\pi} \left(\frac{1}{\lambda_a} - \frac{1}{\lambda_b} \right) \int_{\mathcal{L}} \frac{\bar{u}_n(\hat{\mathbf{r}}, t) (\mathbf{r} - \hat{\mathbf{r}}) \cdot \mathbf{N}(\mathbf{r}, t)}{|\mathbf{r} - \hat{\mathbf{r}}|^2} d\mathcal{L}_{\hat{\mathbf{r}}} \end{aligned} \quad (29)$$

Here \mathcal{L} represents the evolving interface.

For the channel geometry one obtains,

$$P(\mathbf{r}, t) = -\left(\frac{1}{\lambda_a} + \frac{1}{\lambda_b} \right) \mathbf{U}_\infty \cdot \mathbf{r} + \frac{1}{2\pi} \left(\frac{1}{\lambda_a} - \frac{1}{\lambda_b} \right) \int_{\mathcal{L}} \bar{u}_n(\hat{\mathbf{r}}, t) G(\mathbf{r} - \hat{\mathbf{r}}) d\mathcal{L}_{\hat{\mathbf{r}}}, \quad (30)$$

$$\begin{aligned} \frac{1}{2} \left(\frac{1}{\lambda_a} + \frac{1}{\lambda_b} \right) \mathbf{U}_\infty(\mathbf{r}, t) \cdot \mathbf{N} &= \frac{1}{2} \left(\frac{1}{\lambda_a} + \frac{1}{\lambda_b} \right) \bar{u}_n(\mathbf{r}, t) \\ &- \frac{1}{2\pi} \left(\frac{1}{\lambda_a} - \frac{1}{\lambda_b} \right) \int_{\mathcal{L}} \bar{u}_n(\hat{\mathbf{r}}, t) \nabla_{\mathbf{r}} G(\mathbf{r} - \hat{\mathbf{r}}) \cdot \mathbf{N}(\mathbf{r}, t) d\mathcal{L}_{\hat{\mathbf{r}}}, \end{aligned} \quad (31)$$

where

$$G(\mathbf{r} - \hat{\mathbf{r}}) = -\frac{1}{2} \ln \left[\sin^2 \left(\frac{\pi(x - \hat{x})}{l} \right) + \sinh^2 \left(\frac{\pi(y - \hat{y})}{l} \right) \right]. \quad (32)$$

Problems (23),(28),(29) and (23),(30),(31) form a closed system of integro-differential equations which allows to determine position of the interface. In the following section we present results of numerical simulations.

5 Numerical strategy and simulations

The normal advancement of the interface $\mathbf{R} = (x(s, t), y(s, t))$ at the rate V_n is automatically ensured if one sets,

$$\begin{aligned} \frac{\partial x}{\partial t} + V_s \frac{\partial x}{\partial s} &= V_n \frac{\partial y}{\partial s}, \\ \frac{\partial y}{\partial t} + V_s \frac{\partial y}{\partial s} &= -V_n \frac{\partial x}{\partial s}, \end{aligned} \quad (33)$$

where V_s is defined by Eq.(A8), $0 \leq s \leq L(t)$, and $L(t)$ is defined by the relation

$$\frac{dL}{dt} = V_s(s = L(t), t). \quad (34)$$

Eqs. (33) are purely geometrical statements valid for any V_n . The front dynamics is specified by the relation (23), where \bar{u}_n and \bar{P} are defined by Eqs. (28) (29) or Eqs. (30) (31).

Eqs. (33) are considered jointly with the following periodic boundary conditions.
For the source problem,

$$x(0, t) = x(L, t), \quad y(0, t) = y(0, L), \quad x_s(0, t) = x_s(L, t), \quad y_s(0, t) = y_s(L, t). \quad (35)$$

For the channel problem,

$$x(0, t) = x(L, t) + l, \quad y(0, t) = y(0, L), \quad x_s(0, t) = x_s(L, t), \quad y_s(0, t) = y_s(L, t). \quad (36)$$

The boundary conditions should be supplemented by initial conditions,

$$x(s, 0) = x_0(s), \quad y(s, 0) = y_0(s), \quad L(0) = L_0. \quad (37)$$

The quasi-steady nature of Eqs.(28)(30) prevents evaluation of $\bar{u}_n(s, t)$ as a solution of an initial value problem. Yet, $\bar{u}_n(s, t)$ can be successfully calculated through the interactive procedure [10]. As the zeroth approximation one may take $\bar{u}_n^0 = Q/L_0$ for Eq.(28) and, $\bar{u}_n^{(0)} = U_\infty$ for Eq. (30), pertaining respectively to the undisturbed radial and rectilinear flows.

For the source problem the initial conditions are conveniently given in terms of the auxiliary angle $0 \leq \theta < 2\pi$,

$$x_0 = R(\theta) \cos \theta, \quad y_0 = R(\theta) \sin \theta, \quad (38)$$

where the profile $R(\theta)$ is specified as,

$$R(\theta) = R_0 \left[1 + a \left(\cos 5\theta + \frac{1}{3} \sin 13\theta + \frac{1}{10} \cos 27\theta \right) \right]. \quad (39)$$

Note that at $a \ll 1$, $L_0 = 2\pi R_0(1 + O(a^2))$.

For the channel geometry the initial conditions are given in terms of the parameter $0 \leq \psi \leq 1$,

$$x_0 = l(1 - \psi), \quad y_0 = -\frac{al}{2\pi} \left[\frac{1}{2} \sin(2\pi\psi) + \sin(10\pi\psi) \right]. \quad (40)$$

At $a \ll 1$, $L_0 = l(1 + O(a^2))$.

For the source geometry the system (22),(28), (29) does not have an intrinsic length-scale. So

$$r_{ref} = \frac{L_0}{2\pi}, \quad u_{ref} = \frac{Q}{r_{ref}}, \quad t_{ref} = \frac{\phi r_{ref}(F_b - F_a)}{u_{ref}(S_b - S_a)} \quad (41)$$

are utilized as the reference length, velocity, and time scales, respectively. We also set,

$$\nu = \frac{\lambda_a}{\lambda_b}, \quad \gamma = \frac{1}{r_{ref} u_{ref}} \left(\frac{G_b - G_a}{F_b - F_a} \right), \quad (42)$$

which may be regarded as the relative mobility and scaled capillary diffusivity, respectively.

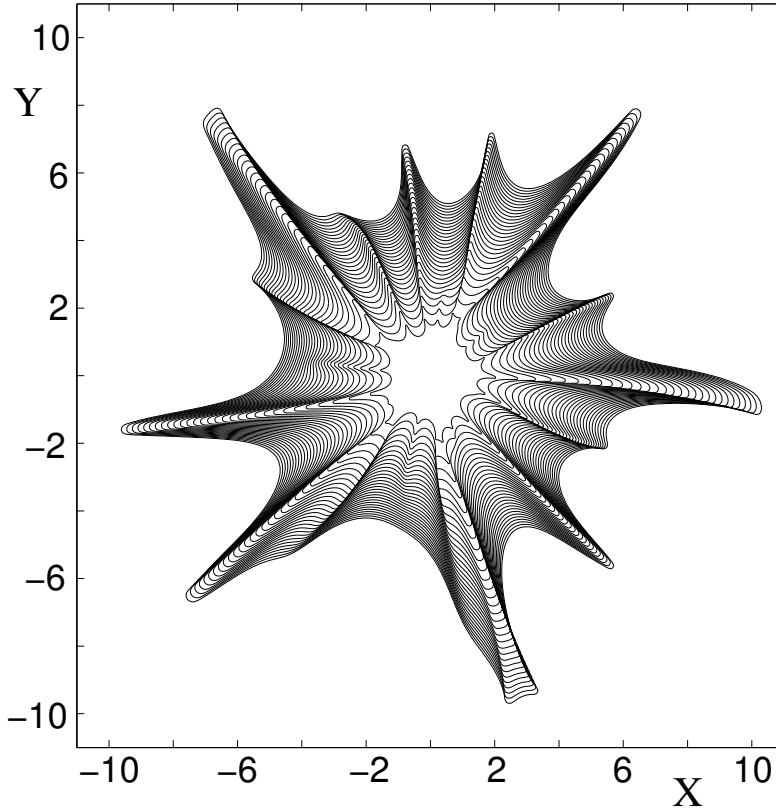


Figure 1: Source geometry. Immiscible displacement front at several consecutive instants of time. $(X, Y) = (x, y)/r_{ref}$. The time-interval between the plotted curves is set at $\Delta t = 4t_{ref}$.

Figure 1 presents results of numerical simulations of the problem (22),(28),(29) with the initial condition (38),(39) at $\nu = 0.125$, $\gamma = 0.001$, and $a = 0.1$.

Note the cusp-leading nature of the emerging fingering structure. This is opposite to the cusp-trailing structure occurring in premixed gas cellular/wrinkled flames [13]. Some of the cusp-tips show a tendency toward swelling and subsequent splitting. Both features are observed in direct numerical simulations of the original Buckley-Leverett model recently undertaken by Riaz and Tchelepi [14],[15].

For the channel geometry the dispersion relation (18) suggests the following set of the length, time, and velocity scales associated with the maximum growth rate of small perturbations,

$$r_{ref} = \frac{2}{u_{ref}} \left(\frac{G_b - G_a}{S_b - S_a} \right) \left(\frac{\lambda_b + \lambda_a}{\lambda_b - \lambda_a} \right), \quad t_{ref} = \frac{2r_{ref}}{\phi u_{ref}} \left(\frac{\lambda_b + \lambda_a}{\lambda_b - \lambda_a} \right), \quad u_{ref} = U_\infty. \quad (43)$$

Figure 2 presents results of numerical simulations of the system (22),(30),(31) for initial-boundary conditions (36), (40) at $\nu = 0.125$, $a = 0.05$ with the channel length $l = 20\pi r_{ref}$.

The incipient dynamics closely follows the initial data. However, with the passage of time the development of primary (small-scale) corrugations slows down giving way to formation

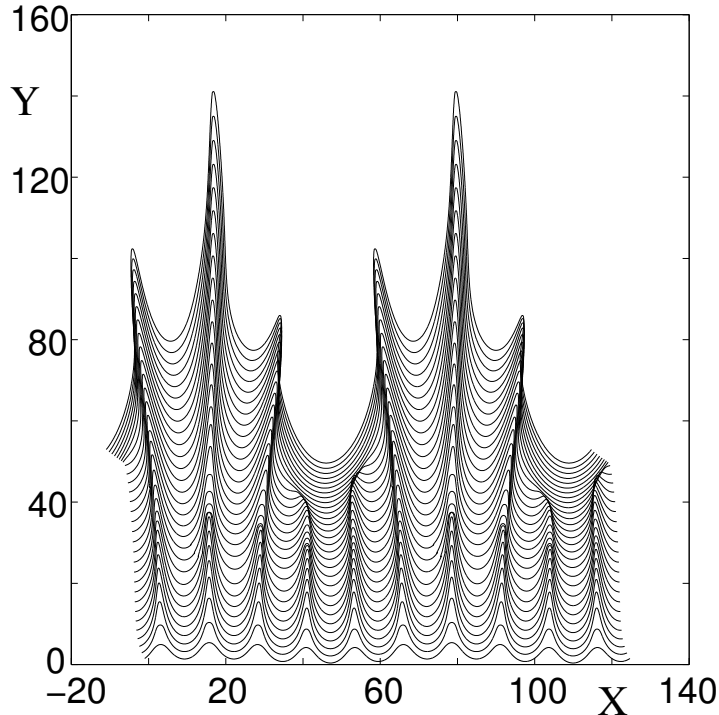


Figure 2: Channel geometry with periodic boundary conditions. Immiscible displacement front at several consecutive instants of time. $(X, Y) = (x, y)/r_{ref}$. The shown configurations correspond to the incipient dynamics over the doubled spatial interval $(2l)$. The time-interval between the plotted curves is set at $\Delta t = t_{ref}$.

of a single cusp-like finger. Such an inverse-cascade behavior is in line with direct numerical simulations [14],[15] and is quite common to many other pattern-forming systems [16],[17],[18].

6 Concluding remarks

Comparison with direct numerical simulations [14],[15] shows that the reduced model (23), though highly extrapolative in nature, captures correctly the salient features of the original Buckley-Leverett model such as cusp-leading fingering, cusp merging and splitting. The found fingering pattern is quite distinct from the coral-like fingering rendered by the recently derived model for miscible displacement [11] (Fig. 3). In the miscible system the dissipation of short-wavelength disturbances is provided by the interfacial curvature rather than the stretch. The visual dissimilarity in pattern forming pictures however is not exactly in line with experimental observations where the qualitative distinction between fingering patterns in miscible and immiscible displacements is not at all obvious, contrary to theoretical-numerical predictions. One may compare the pictures in experimental studies [19][20] dealing with immiscible and miscible displacement, respectively. This difficulty suggests that, for all its success in covering various aspects of immiscible displacement, the Buckley-Leverett model is apparently incomplete, and requires incorporation of some additional ingredients related

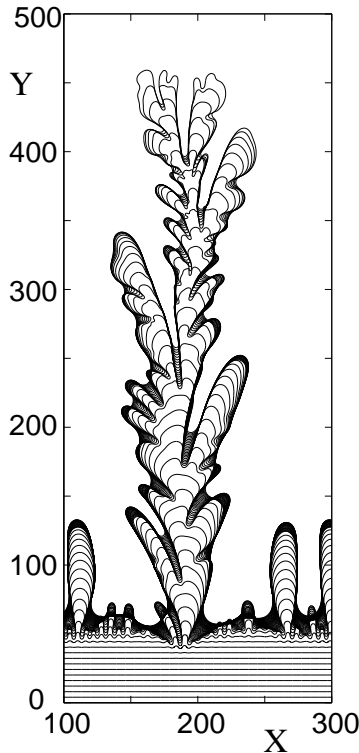


Figure 3: Miscible displacement front at several consecutive instants of time. For conditions see [11].

to capillary effects. A more fundamental first-principal approach to modeling two-phase immiscible flows is needed [2].

Acknowledgments The work of IB and GS was supported in part by the Alberta Research Council, the US-Israel Binational Science Foundation (Grant 2006-151), and the Israel Science Foundation (Grant 350/05), and the European Community Program RTN-HPRN-CT-2002-00274. The work of PG was partially supported by NSF grant DMS-0554775. GS also thanks Michael Frankel for helpful discussions.

Appendix A Derivation of Eq.(22)

In order to make the analysis tractable it is convenient to rewrite Eqs.(1), (2) in terms of front-attached (intrinsic) coordinates, instantaneously normal and parallel to the displacement front. Details can be found in [21]. In terms of intrinsic coordinates the position vector of a reference point reads,

$$\mathbf{r}(n, s, t) = \mathbf{R}(s, t) + n\mathbf{N}(s, t). \quad (\text{A1})$$

Here, s is an arclength of the interface and n is a distance from the reference point to the interface in the normal direction. \mathbf{N} is a unit normal vector directed towards the fluid ahead

of the interface. Thus, the interface is described by \mathbf{r} evaluated at $n = 0$, that is by \mathbf{R} . In the intrinsic coordinates the flow field may then be written as,

$$\mathbf{u} = u_n \mathbf{N} + u_s \mathbf{T}, \quad (\text{A2})$$

where u_n and u_s are normal and tangent components of the fluid flow and $\mathbf{T} = \partial \mathbf{R} / \partial s$ is the unit tangent vector. The unit normal and unit tangent vectors are related by Frenet formulas,

$$\frac{\partial \mathbf{N}}{\partial s} = \mathcal{K} \mathbf{T}, \quad \frac{\partial \mathbf{T}}{\partial s} = -\mathcal{K} \mathbf{N}, \quad (\text{A3})$$

where \mathcal{K} is the curvature of the interface. Therefore,

$$\nabla = \mathbf{N} \frac{\partial}{\partial n} + \frac{\mathbf{T}}{1 + n\mathcal{K}} \frac{\partial}{\partial s}. \quad (\text{A4})$$

In terms of intrinsic coordinates (s, n) Eqs.(1)(2) read,

$$\begin{aligned} \phi \left(\mathcal{D}_t S - V_n \frac{\partial S}{\partial n} \right) + u_n \frac{\partial F(S)}{\partial n} + \frac{u_s}{1 + n\mathcal{K}} \frac{\partial F(S)}{\partial s} = \\ \frac{\partial}{\partial n} \left(D(S) \frac{\partial S}{\partial n} \right) + \frac{\mathcal{K} D(S)}{1 + n\mathcal{K}} \frac{\partial S}{\partial n} + \frac{1}{1 + n\mathcal{K}} \frac{\partial}{\partial s} \left(\frac{D(S)}{1 + n\mathcal{K}} \frac{\partial S}{\partial s} \right), \end{aligned} \quad (\text{A5})$$

$$\frac{\partial u_n}{\partial n} + \frac{\mathcal{K}}{1 + n\mathcal{K}} u_n + \frac{1}{1 + n\mathcal{K}} \frac{\partial u_s}{\partial s} = 0. \quad (\text{A6})$$

Here, $V_n = \partial \mathbf{R} / \partial t \cdot \mathbf{N}$ and $V_s = -\partial \mathbf{R} / \partial t \cdot \mathbf{T}$ are normal and tangent components of the velocity of the interface, and \mathcal{D}_t is the material time derivative defined as,

$$\mathcal{D}_t = \frac{\partial}{\partial t} + V_s \frac{\partial}{\partial s}. \quad (\text{A7})$$

The normal and tangent components of the interface velocity are related by transport identity,

$$\frac{\partial V_s}{\partial s} = \mathcal{K} V_n. \quad (\text{A8})$$

By our assumption the interface is weakly curved, that is $\mathcal{K} \sim \varepsilon$ with $\varepsilon \ll 1$. This suggests a natural scaling,

$$\xi = \varepsilon s, \quad \tau = \varepsilon t, \quad \varkappa = \mathcal{K} / \varepsilon. \quad (\text{A9})$$

Moreover, the mild mobility contrast validates the assumption that velocity field depends only on slow variables that is,

$$\mathbf{u} = \mathbf{u}(\varepsilon n, \xi, \tau). \quad (\text{A10})$$

Since the saturation S is expected to approach its limiting values (S_a, S_b) exponentially fast, one can asymptotically replace the system (A5) (A6) by its expansion applied to diffusive layer $|n| \sim 1$ and seek the solution in the form,

$$S = S^{(0)}(n, \xi, \tau) + \varepsilon S^{(1)}(n, \xi, \tau) + O(\varepsilon^2), \quad V_n = V^{(0)} + \varepsilon V^{(1)} + O(\varepsilon^2) \quad (\text{A11})$$

Within this approximation the equation (A5) for the saturation S taking into account incompressibility condition (A6) reads,

$$\begin{aligned} & -\phi V_n \frac{\partial S}{\partial n} + \varepsilon \phi \mathcal{D}_\tau S^{(0)} + \bar{u}_n \frac{\partial F(S)}{\partial n} + \varepsilon \bar{u}_s \frac{\partial F(S^{(0)})}{\partial \xi} - \varepsilon n \left(\varkappa \bar{u}_n + \frac{\partial \bar{u}_s}{\partial \xi} \right) \frac{\partial F(S^{(0)})}{\partial n} = \\ & = \frac{\partial}{\partial n} \left(D(S) \frac{\partial S}{\partial n} \right) + \varepsilon \varkappa D(S^{(0)}) \frac{\partial S^{(0)}}{\partial n} + O(\varepsilon^2). \end{aligned} \quad (\text{A12})$$

Here,

$$\bar{\mathbf{u}}(\xi, \tau) = \mathbf{u}(n = 0, \xi, \tau), \quad (\text{A13})$$

and \mathcal{D}_τ is the scaled material time derivative.

Integrating Eq.(A12) in n from $-\infty$ to ∞ we have,

$$\begin{aligned} & -\phi V_n (S_a - S_b) + \phi \mathcal{D}_\tau \langle S^{(0)} \rangle_n + \bar{u}_n (F_a - F_b) + \varepsilon \bar{u}_s \frac{\partial}{\partial \xi} \langle F(S^{(0)}) \rangle_n \\ & - \varepsilon \left(\varkappa \bar{u}_n + \frac{\partial \bar{u}_s}{\partial \xi} \right) \left\langle n \frac{\partial F(S^{(0)})}{\partial n} \right\rangle_n = \varepsilon \varkappa (G_a - G_b), \end{aligned} \quad (\text{A14})$$

where F_a, F_b, G_a, G_b are as in Section 4 and $\langle S \rangle_n$ is average saturation in the following sense,

$$\langle S \rangle_n = \lim_{\delta \rightarrow 0} S_\delta, \quad S_\delta(\xi, \tau) = \int_0^{1/\delta} (S(n, \xi, \tau) - S_a) dn + \int_{-1/\delta}^0 (S(n, \xi, \tau) - S_b) dn. \quad (\text{A15})$$

The quantity $\langle S \rangle_n$ was first introduced in [22] in the context of the nonlinear filtration problem. We also note that

$$\left\langle n \frac{\partial S}{\partial n} \right\rangle_n = -\langle S \rangle_n. \quad (\text{A16})$$

Recombining terms in (A14) and taking into account identity (A16) we obtain

$$\phi V_n = \frac{F_b - F_a}{S_b - S_a} \bar{u}_n - \frac{\varepsilon}{S_b - S_a} R_\varepsilon, \quad (\text{A17})$$

where

$$R_\varepsilon = (G_b - G_a) \varkappa + \phi \mathcal{D}_\tau \langle S^{(0)} \rangle_n + \varkappa \bar{u}_n \langle F(S^{(0)}) \rangle_n + \frac{\partial}{\partial \xi} (\bar{u}_s \langle F(S^{(0)}) \rangle_n). \quad (\text{A18})$$

Setting $\varepsilon = 0$ in (A17) we have,

$$\phi V_n^{(0)} = \frac{F_b - F_a}{S_b - S_a} \bar{u}_n. \quad (\text{A19})$$

Thus, in the zeroth approximation the problem (A12) reduces to,

$$-\frac{F_b - F_a}{S_b - S_a} \bar{u}_n \frac{\partial S^{(0)}}{\partial n} + \bar{u}_n \frac{\partial F(S^{(0)})}{\partial n} = \frac{\partial}{\partial n} \left(D(S) \frac{\partial S^{(0)}}{\partial n} \right). \quad (\text{A20})$$

Integrating (A20) twice in n , we obtain,

$$\langle F(S^{(0)}) \rangle_n - \frac{F_b - F_a}{S_b - S_a} \langle S^{(0)} \rangle_n = -\frac{G_b - G_a}{\bar{u}_n}. \quad (\text{A21})$$

Another useful property comes from the observation that $S^{(0)}$ is a function of single variable $\eta = \bar{u}_n n$. In terms of η Eq.(A20) reads,

$$-\frac{F_b - F_a}{S_b - S_a} \frac{\partial S^{(0)}}{\partial \eta} + \frac{\partial F(S^{(0)})}{\partial \eta} = \frac{\partial}{\partial \eta} \left(D(S^{(0)}) \frac{\partial S^{(0)}}{\partial \eta} \right). \quad (\text{A22})$$

Note, that

$$\langle S^{(0)} \rangle_\eta = \bar{u}_n \langle S^{(0)} \rangle_n \quad (\text{A23})$$

and $\langle S^{(0)} \rangle_\eta$ is independent of ξ and τ . In addition, scaled in terms of (A9), the transport identity (A8) together with (A19) imply,

$$\varkappa = \phi \frac{S_b - S_a}{F_b - F_a} \frac{1}{\bar{u}_n} \frac{\partial V_s}{\partial \xi} + O(\varepsilon) \quad (\text{A24})$$

Substituting (A7) (A21), (A23) and (A24) into (A18), after simple algebraic manipulations, we obtain,

$$\begin{aligned} R_\varepsilon &= \phi \langle S^{(0)} \rangle_\eta \frac{\partial}{\partial \tau} \left(\frac{1}{\bar{u}_n} \right) + \phi \langle S^{(0)} \rangle_\eta \frac{\partial}{\partial \xi} \left(\frac{V_s}{\bar{u}_n} \right) \\ &+ \left(\frac{F_b - F_a}{S_b - S_a} \langle S^{(0)} \rangle_\eta - (G_b - G_a) \right) \frac{\partial}{\partial \xi} \left(\frac{\bar{u}_s}{\bar{u}_n} \right). \end{aligned} \quad (\text{A25})$$

So far the position of the interface has not been fixed. Therefore, we have freedom to chose the position of the set corresponding to $n = 0$. Since $\langle S^{(0)} \rangle_\eta$ is constant we define the set $n = 0$ by the following condition (see also (17)),

$$\langle S^{(0)} \rangle_\eta = 0. \quad (\text{A26})$$

With this choice of the reference position Eq.(A25) takes a particularly simple form,

$$R_\varepsilon = - (G_b - G_a) \frac{\partial}{\partial s} \left(\frac{\bar{u}_s}{\bar{u}_n} \right). \quad (\text{A27})$$

Finally, substituting (A27) into (A17) we obtain,

$$\phi V_n = \frac{F_b - F_a}{S_b - S_a} \bar{u}_n + \varepsilon \frac{G_b - G_a}{S_b - S_a} \frac{\partial}{\partial \xi} \left(\frac{\bar{u}_s}{\bar{u}_n} \right). \quad (\text{A28})$$

Returning to the original (unscaled) variables s and t in (A28), one finally ends up with Eq.(22).

Equation (23) pertains to the two dimensional geometry. In the extension over three dimensions, as may be shown, the relaxation term $\frac{\partial}{\partial s} \left(\frac{1}{\bar{u}_n} \frac{\partial \bar{P}}{\partial s} \right)$ of Eq.(23) is replaced by $-\mathbf{N} \cdot \text{curl} ((\nabla P \times \mathbf{N}) / \bar{u}_n)|_{n=0}$.

References

- [1] R. A. Wooding and H. J. Morel-Seytoux, *Ann. Rev. Fluid Mech.* 8, 233 (1976).
- [2] G. M. Homsy, *Ann. Rev. Fluid Mech.* 19, 271 (1987).
- [3] G. I. Barenblatt, V. M. Entov, and V. M. Ryzhik, *Theory of Unsteady Filtration of Liquid and Gases (in Russian)*, Nedra, Moscow, 1972.
- [4] G. I. Barenblatt, V. M. Entov, and V. M. Ryzhik, *Theory of Fluid Flow through Natural Rocks*, Kluwer Acad. Publ. Dordrecht, 1990.
- [5] J. Hagort, *Soc. Petr. Eng. J.* 14, 63 (1974).
- [6] Y. C. Yortsos and A. B. Huang, SPE 12692, *Soc. Petr. Eng.*, Dallas, Tex., 1984.
- [7] G. R. Jerauld, I. C. Nitsche, G. F. Teletske, H. T. Davis, and L. E. Scriven, SPE 12691, *Soc. Petr. Eng.*, Dallas, Tex., 1984.
- [8] G. R. Jerauld, H. J. Davis, and L. E. Scriven, SPE 13164, *Soc. Petr. Eng. Dallas, Tex.*, 1984.
- [9] E. D. Chikhliwala, and Y. C. Yortsos, SPE 14367, *Soc. Petr. Eng. Dallas, Tex.*, 1985.
- [10] I. Brailovsky, A. Babchin, M. Frankel, and G. Sivashinsky, *Transp. Porous Media* 63, 363 (2006).
- [11] I. Brailovsky, A. Babchin, M. Frankel, and G. Sivashinsky, *Phys. Lett. A* 369, 212 (2007).
- [12] V. M. Ryzhik, I. A. Charni, and C. Chzhun-Syan, *Izv. AN SSR, OTN, Mekh. i Mash. (in Russian)* 1, 121 (1961).
- [13] G. I. Sivashinsky, *Ann. Rev. Fluid Mech.* 15, 179 (1983).
- [14] A. Riaz, and H. A. Tchelepi, *Phys. Fluids* 18, 014104 (2006).
- [15] A. Riaz, and H. A. Tchelepi, *Transp. Porous Media* 64, 315 (2006).
- [16] R. A. Wooding, *J. Fluid Mech.* 39, 477 (1969).
- [17] P. G. Saffman, and G. I. Taylor, *Proc. R. Soc. London Ser. A*, 245, 31 (1958).
- [18] M. Q. López-Salvans, J. Casademunt, G. Iori, and F. Sagnés, *Physica D*, 164, 127 (2002).
- [19] J. P. Stokes, D. A. Weitz, J. P. Gollub, A. Dougherty, M. O. Robbins, P. M. Chaikin, and H. M. Lindsay, *Phys. Rev. Lett.* 57, 1718 (1986).
- [20] L. Paterson, *Phys. Fluids* 28, 26 (1985).
- [21] M. E. Gurtin, *Thermomechanics of Evolving Phase Boundaries in the Plane*. Oxford Univ. Press, 1993.
- [22] S. A. Vakulenko and I. A. Molotkov, *J. Appl. Math. Mech.* 61, 103 (1997).